Interactive Planning of Cryotherapy Using Physics-Based Simulation

Hugo TALBOT [a,b,1], Myriam LEKKAL [a], Remi BESSARD-DUPARC [a] and Stephane COTIN [a]

[a] *SHACRA team, Inria, France*
[b] *ASCLEPIOS team, Inria, France*

Abstract. Cryotherapy is a rapidly growing minimally invasive technique for the treatment of certain tumors. It consists in destroying cancer cells by extreme cold delivered at the tip of a needle-like probe. As the resulting iceball is often smaller than the targeted tumor, a key to the success of cryotherapy is the planning of the position and orientation of the multiple probes required to treat a tumor, while avoiding any damage to the surrounding tissues. In order to provide such a planning tool, a number of challenges need to be addressed such as fast and accurate computation of the freezing process or interactive positioning of the virtual cryoprobes in the pre-operative image volume. To address these challenges, we present an approach which relies on an advanced computational framework, and a gesture-based planning system using contact-less technology to remain compatible with a use in a sterile environment.

Keywords. Cryotherapy, planning, interaction, simulation

1. Introduction

Cryosurgery (also called cryoablation or cryotherapy) is a clinical technique that has been introduced to treat prostate cancers in the early 1960s. It is based on the Thompson-Joule principle, and works by decompressing very rapidly a gas (usually argon) through a needle-like probe. Cryoprobes are small, hollow, cylindrical devices of about 1.5 mm in diameter, and are inserted into the tumor during laparoscopic surgery or percutaneously under image guidance. As the argon flows through the needle, a ball of ice crystals forms around the tip of the probe, thus immediately leading to cellular death of the surrounding tissues. Only guided by CT or MR images, radiologists might carry out several treatment cycles to freeze the entire tumor to a temperature of 233K to 248K. This technique has been applied to treat many kinds of tumors, such as breast cancer, primary or metastatic liver neoplasms, renal, lung, pancreas, and prostate cancer. The volume of the iceball must be slightly larger than the volume of tumor to ensure the effectiveness of cryosurgery but minimize freezing damage to nearby healthy tissue. Knowing that there are about 6 different types of cryoprobes each producing a different iceball size and shape, the size and shape of the iceball produced by a single probe can vary significantly.

[1] Corresponding Author: E-mail: hugo.talbot@inria.fr.

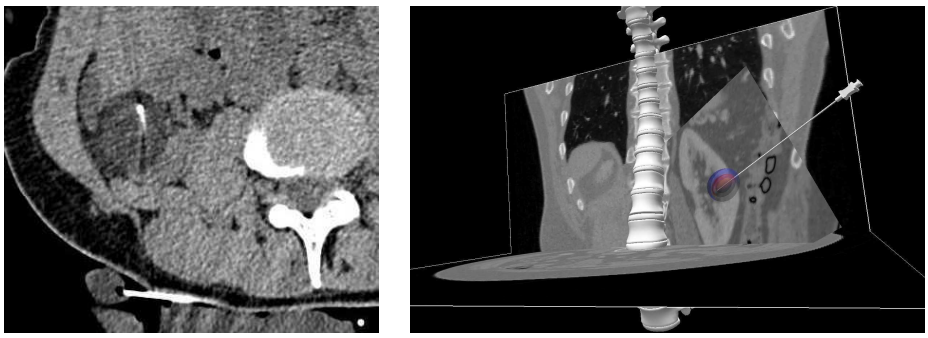

(a) (b)

Figure 1. (a) CT image of a kidney treated with two Ice-Sphere cryoprobes. (b) Screenshot of our framework mixing patient data and cryosurgery simulation.

To guaranty an optimal tumor ablation, a very careful planning must be performed to define the best position for each probe as well as the type of probe. This planning is currently done qualitatively, based on experience, and can take several hours, with a result that is often different for the expected one. To solve this important limitation of cryotherapy, a few planning systems have been proposed in the literature. Currently, commercial systems are nearly non existent, and emerging tools are limited to a visualization of the isotherms obtained for each probe in ideal conditions (usually in a gel). They do not account for any influence of the soft tissue properties, the presence of blood vessels, or the combined effect of multiple probes highlighted in [10]. As a consequence, large safety margins over 5 mm are defined, as detailed in [5].

More advanced approaches have been proposed recently in the literature. They essentially rely on the same equation describing the heat diffusion through soft tissues [11,3,2]. The main criticism of all these different approaches is that they do not address some key requirements for being used in clinical routine. For instance, the computation times reported by Chen *et al.* [3] is of about 2 days of computation for a freezing cycle of 10 minutes, and all of the proposed methods require a significant pre-processing of the medical images to segment, label and mesh the different tissue types.

In this paper, we introduce three main contributions, all aimed at bringing cryotherapy simulation closer to requirements for clinical use. First, our framework (see Fig. 1b) proposes an innovative simulation directly based on medical images, sparing any segmentation, reconstruction and meshing step. Our physics-based simulation can predict the synergistic effect of multiple cryoprobes detailed in [10]. Second, the multiresolution and GPU-based approach significantly reduces computation times compared to the state-of-the-art, making it compatible with a clinical use, which has never been done till now. Third, our framework allows a gesture-based planning system using contact-less technology to remain compatible with a use in a sterile environment. An evaluation using clinical data finally supports our contribution as a significant step forward in the context cryotherapy.

2. Methods

2.1. Numerical Simulation of Cryosurgery

Heat transfer model: The two main models estimating the heat transfer in perfused tissue are the Pennes' model [7] and the Wulff's model [9], both based on the enthalpy method. Front tracking methods can also be used to model heat propagation. However, these tracking methods use non-physiological parameters. In this work, we rely on the Pennes' model that assumes a constant blood temperature. The heat transfer can then be described by the following equation:

$$\rho_t c_t \frac{\partial T}{\partial t} = div(k_t \nabla T) + W_b c_b \ (T_a - T) + Q_m \tag{1}$$

where T is the temperature of the living tissue, ρ_t, k_t and c_t are, respectively, the density, the thermal conductivity and specific heat of the tissue. W_b is the perfusion rate, c_b the specific heat of the blood and T_a is the temperature of the arterial blood. Q_m is the metabolic heat generation.

In this paper, our simulation of thermal diffusion is first compared against experimental data and then using patient-specific images. In both cases, the parameters used in our simulation are the ones presented in [11].

Numerical Approach: Our heat transfer model is implemented using the Finite Element method. Starting from medical images (CT or MR), we define a region of interest around the tumor which is then discretized as a regular 10×10 cm grid of adjustable resolution. Cells of the grid (hexahedra) are further decomposed into regular tetrahedra to better match the shape and resolution of the virtual probe located within the grid. This fine mesh of tetrahedral elements is used to numerically solve the Eq. 1 to reduce numerical errors. To solve the time dependent equation, a full explicit time integration scheme with a Backward Differentiation (noted "Explicit-BDF" solver) is chosen. Since it is an explicit formulation, we obtain a diagonal system ($\mathbf{D}T = b$), that can be solved easily, without a linear solver. A time step of $dt = 0.1$ s is chosen to ensure computational stability and the freezing cycle usually lasts about 10 minutes. Our integration scheme can be written as follows:

$$T_{t+\Delta t} = \frac{1}{3}\left(4 \cdot T_t - T_{t-\Delta t}\right) + \frac{2\,\Delta t}{3} \cdot (\mathbf{D}^{-1} b) \tag{2}$$

Tissue Domain Boundary Conditions: Using a weak formulation for the integration of diffusion term in Eq. 1 leads to zero Neumann boundary conditions in the orthogonal direction of the surface. Denoting t as the surface triangles, we have:

$$\sum_t \frac{k_t A}{3} (\nabla T \cdot \mathbf{n}) = 0 \tag{3}$$

Needle Boundary Conditions: Our simulation also needs to account for the freezing effect due to the cryoprobe. A second boundary condition is introduced to model this negative heat source, as detailed in Eq. 4:

$$-k\frac{\partial T}{\partial n}\bigg|_{surf} = h_\infty\,(T_\infty - T) \tag{4}$$

where h_∞ is the needle convection coefficient, T_∞ is the free-stream temperature of the probe, and subscript *surf* denotes triangles circumscribing the needle surface. This boundary condition has been adapted so that all types of cryoprobes can be simulated.

GPU Implementation: Due to the extreme fineness of cryoprobes, a very fine grid must be used: the edge size has to remain below the probe diameter $dx < 1.47$ mm. In our simulations, we use $dx = 1.25$ mm. The use of larger elements would misrepresent the needle boundary conditions, thus resulting in an incorrect (larger) iceball due to a numerical increase of the freezing effect. The choice of a fine grid preserve accuracy but implies huge computation costs. Computational efficiency therefore becomes a major issue for our cryosurgery simulation dedicated to clinical routine.

Considering this computation cost problem and the low complexity of the Pennes' equation, GPU implementation seems an appropriate solution. GPU computing consists in using all the multi-processors of the graphics processing unit in order to carry out highly parallel tasks. The complexity of GPU computing results in optimally distributing these independent tasks (threads) and minimizing the memory access latency. In our work, the GPU version of our algorithm has been developed using CUDA toolkit dedicated to to NVidia's GPUs. In the Pennes' equation, strong neighboring dependencies of the diffusion term $div(k_t \cdot \nabla T)$ make its implementation on GPU very challenging. In a parallel computation, this algorithm can lead to writing conflicts: two threads solving two adjacent edges could write on the same point simultaneously. Using recent CUDA versions enables to overcome this issue, but we rely on a more powerful solution based on [1]. Originally designed for solving non-linear elasticity problems, Allard et al. present a set of GPU algorithms that we adapt to cryosurgery simulation. The GPU implementation of the additional terms (metabolic and arterial heat) is more straightforward and do not require other advanced implementation technique.

2.2. Interaction and Visualization

Interactive planning: We were given the opportunity to observe cryoablation procedures to evaluate the use of current technologies in the operating room and how they affect the efficiency of the procedure. We found that interventional radiologists rely on verbal instructions to communicate with assistants (located outside of the operating room for radiation safety). This communication involves essentially the selection of the optimal pre-operative image planes, or the review of the planned strategy (with a visualization of the trajectory of the cryoprobes). It is obvious that communicating image manipulation instructions is a lot less efficient than doing it directly using a mouse for instance. However, this is rarely possible in the operating room: contacts with non sterile objects are prohibited, and when performing the cryotherapy under MR guidance, computer equipment must remain outside of the room.

Our solution to this problem is to rely on gesture interaction using contactless technology [6], allowing the interventional radiologist to review pre-operative images or use the cryotherapy simulation « in situ » while remaining sterile [8]. While the Kinect (Mi-

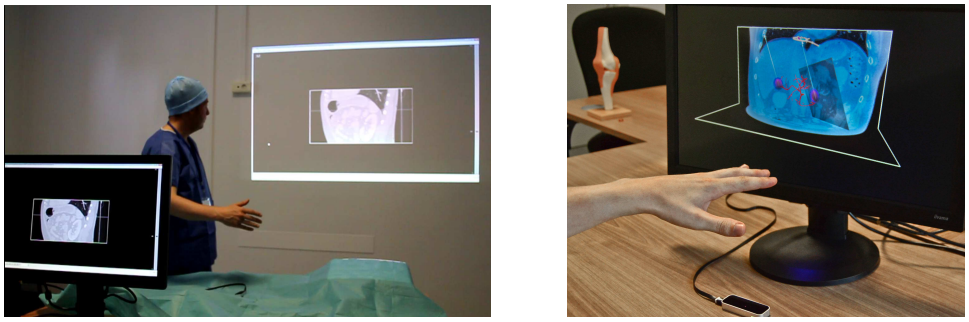

(a) (b)

Figure 2. Touchless gesture : (a) interactive sterile browsing of medical images using the Leap Motion, and (b) control of the trajectory of the cryoprobes using gestures

crosoft) has been until now the preferred choice for such type of control [4], we chose the Leap Motion device[2] for its added accuracy and the robustness of the finger tracking. We also believe that finger gestures are not only more intuitive for the surgeon but also decrease Gorilla Arm effect (user fatigue) compared to hand/arm gestures.

Gesture vocabulary: Accurate finger tracking is not directly needed for efficient interactive review and planning of the procedure. A higher-level "language" needs to be developed, by creating a gesture vocabulary based on finger postures. Our focus in this work is to find the specific gestures that make this specific application more efficient. This, by considering the semantic interpretation of the gestures in order to make them easy to remember and perform by the surgeon.

Visualization : With this interaction technique, we allow the surgeon to navigate through the preoperative images (see Fig. 2a) but also manipulate the cryoprobes using gestures and visualize their positions so that the iceball covers the entire tumor (see Fig. 2b). As a result, we can provide a better and direct control of the planning software in a faster, more natural way.

3. Results

To validate our simulation, we perform a series of experiments using Ice-Rod probes immersed in water. CT scans of the same ice balls were obtained at the end of the freezing cycle in order to have a three-dimensional model. The ice balls were then manually segmented. For the experimental tests into the water, the ambient temperature is set to 23^oC and the metabolic heat, as well as the blood perfusion rate, are set to zero. A first experiment using one probe is conducted to evaluate diffusion parameters (see the resulting iceball in Fig 3a). Based on this parameter estimation, an experiment using two probes (see Fig. 3b) is carried out to assess the ability of our framework to account for the

[2]For more information about Leap Motion technology: please see `www.leapmotion.com`.

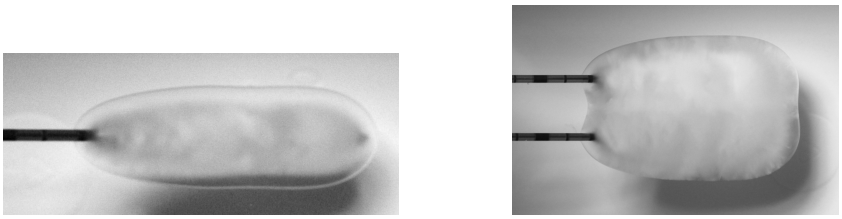

(a) (b)

Figure 3. (a) Pictures of the ice ball of one Ice-Rod needle and (b) resulting from the synergistic effect of two cryoprobes.

crucial synergistic effect presented in [10]. The Hausdorff distances measured between the segmented and the simulated iso-surface are given in Table 1 and represented in Fig. 4. For both *in vitro* cases, it appears that the maximum distance remain below 2 mm while requiring less than 30 seconds of computation.

After validating our model on *in vitro* data, we perform (retrospectively) a preliminary test on patient-data. We select a patient with straightforward parametrization: heterogeneity between healthy and tumor tissues is not distinctly noticeable from medical images (see Fig. 1). Defining homogeneous properties in our computation volume seems therefore relevant. The model parameters used in this simulation are the ones presented in [11]. Again, the iceball resulting from the simulation is compared with the segmented iceball. Hausdorff distance maps give very encouraging results (see Fig. 5), and certainly a lot more accurate than what could be obtained using the manufacturer iso-surfaces.

Table 1. Hausdorff distance (in mm) computed between ice balls from segmentation and simulation.

	in vitro (water)		Patient data
	1 probe	2 probes	
Mean	0.441	0.271	0.655
Max	1.108	1.352	2.347

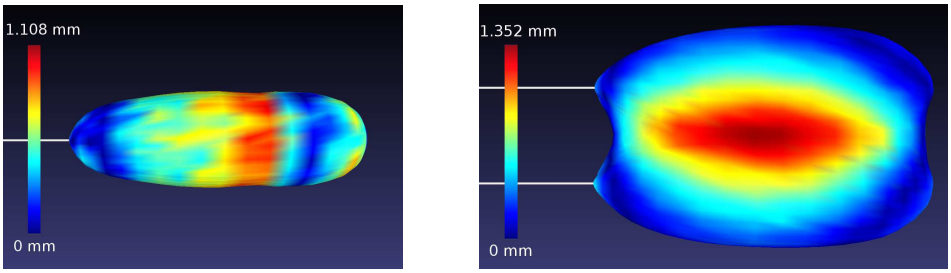

(a) (b)

Figure 4. Hausdorff distance computed between the segmented and simulation based iso-surfaces: (a) using one and (b) two Ice-Rod cryoprobes.

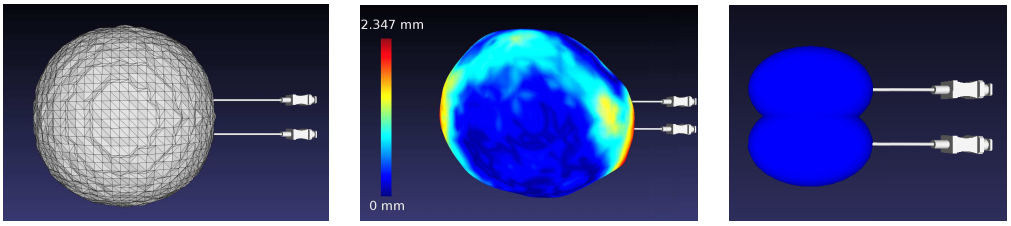

(a) (b) (c)

Figure 5. Iso-surface obtained from: (a) simulation, (b) patient-specific data (with Hausdorff distance) and (c) manufacturer.

4. Conclusion

In this paper, we present an interactive planning framework for cryotherapy, compatible with the requirements set by interventional radiologists. Using contact-less technology, virtual cryoprobes can be interactively positioned in a sterile environment. Based on a fast yet accurate GPU implementation, the resulting iceball is computed in less that 30 s, outperforming previous work. This framework therefore allows to significantly decrease the safety margin by taking into account the synergistic effect of multi-cryoprobes with computation times consistent with clinical application while preserving accuracy. In this context, our numerical strategies, such as the choice of GPU computing or grid-based finite element approach, prove to be relevant. A video is attached to this paper in order to better discover this interactive planning framework.

References

[1] J. Allard, H. Courtecuisse, and F. Faure. *Implicit FEM Solver on GPU for Interactive Deformation Simulation*. Elsevier, 2011.

[2] D.J. Blezek, D.G. Carlson, L.T. Cheng, J.A. Christensen, M.R. Callstrom, and B.J. Erickson. Cell accelerated cryoablation simulation. *Computer Methods and Programs in Biomedicine*, 98(3):pp. 241–252, 2010.

[3] C.W. Chen, H.S. Kou, H.E. Liu, C.K. Chuang, and L.J. Wang. Computer assisted simulation model of renal tumor cryosurgery. *Heat Transfer 2009*, 3:pp. 741–748, 2009.

[4] L.C Ebert, G. Hatch, M.J. Thali, and S. Ross. Invisible touch-control of a dicom viewer with finger gestures using kinect depth camera. *Journal of Forensic Radiology and Imaging*, 2012.

[5] C. Georgiades, R. Rodriguez, E. Azene, C. Weiss, A. Chaux, and *et al.* Determination of the non-lethal margin inside the visible "ice-ball" during percutaneous cryoablation of renal tissue. *Cardiovasc Intervent Radio*, pages pp. 1–8, 2012.

[6] R. Jhonson, K. O'Hara, A. Sellen, C. Cousins, and A. Criminisi. Exploring the potential for touchless interaction in image-guided interventional radiology. In *CHI 2011*.

[7] H.H. Pennes. Analysis of tissue and arterial blood temperatures in the resting human forearm. *Journal of applied physiology*, 1(2):pp. 93–122, 1948.

[8] J.P. Wachs, H.I. Stern, Y. Edan, M. Gillam, J. Handler, C. Feied, and M. Smith. A gesture-based tool for sterile browsing of radiology images. *Journal of the American Medical Informatics Association*, 15(2):pp. 321–323, May/June 2008.

[9] W. Wulff. The energy conservation equation for living tissue. *Biomedical Engineering, IEEE Transactions on*, (6):pp. 494–495, 1974.

[10] J.L Young. Are multiple cryoprobes additive or synergistic in renal cryotherapy? *Urology*, 2011.

[11] J. Zhang, G.A. Sandison, J.Y. Murthy, and L.X. Xu. Numerical simulation for heat transfer in prostate cancer cryosurgery. *J Biomech Eng*, 127(2):pp. 279–294, April 2005.